Carlos Alberto Galarza, Matias Orlando Miranda, and Darío Jorge Roberto Duarte*

Laboratorio de Estructura Molecular y Propiedades, Universidad Nacional del Nordeste.
Instituto de Química Básica y Aplicada del Nordeste Argentino (IQUIBA-NEA). Corrientes, Argentina.
carlosgalarza333@gmail.com, matiorly@hotmail.com, djr_duarte@hotmail.com.

***Corresponding author:** djr_duarte@hotmail.com.

Received: 09/10/2024. **Last Review:** 06/04/2025. **Accepted:** 27/05/2025.

Applied and Analytical

Detection and Characterization of Halogen Bonds by UV-Vis Spectrophotometry and Molecular Modelling

Abstract

This study investigates halogen bonds (XBs) in bromine-acetone complexes (Br_2•••Ac) using UV-Vis spectrophotometry and computational methods. Electronic structure calculations, including geometry optimizations and excited-state calculations, were carried out using the Gaussian 16 program. Time-Dependent Density Functional Theory (TD-DFT) method, with the M06-2X functional and def2-TZVP basis set, was employed to determine absorption energies corresponding to HOMO→LUMO transitions. Acetone solvation was simulated using the Polarizable Continuum Model (PCM). Exper-imental UV-Vis spectra of gaseous Br_2 revealed two absorption peaks at 238 nm ($\lambda_{1,exp}$) and 454 nm ($\lambda_{2,exp}$). Upon dissolution in acetone, $\lambda_{2,exp}$ underwent a hypsochromic (blue) shift, reaching 395 nm and 365 nm at 0.04 and 0.01 M Br_2, respectively. This shift is attributed to XB formation, supported by theoretical spectra showing peaks at 390 nm (Br_2•••Ac) and 360 nm (Ac•••Br_2•••Ac). The 238 nm peak in Br_2(g) is associated with Br_2•••Br_2 complexes, corroborated by a theoretical peak at 240 nm. A single peak at 415 nm in Br_2(g) diluted in air is attributed to Br_2•••N_2 complexes, with a corre-sponding theoretical peak at 417 nm. Theoretical and experimental data align well, validating the methodology and highlighting the role of XBs and electronic transitions in modulating Br_2 spectrophotometric properties.

Keywords: Halogen bonds; UV-Vis spectrophotometry; molecular modelling; electronic transitions.

Detección y caracterización de enlaces halógenos por medio de espectrofotometría UV-Vis y modelado molecular

Resumen

Este estudio analiza los enlaces de halógeno (XBs) en complejos de bromo y acetona (Br_2•••Ac) mediante espectrofotometría UV-Vis y métodos computacionales. Se realizaron cálculos de estructura electrónica, optimización geométrica y estados excitados con el programa Gaussian 16. Se empleó el método de la teoría del funcional de la densidad dependiente del tiempo (TD-DFT), con el funcional M06-2X y la base def2-TZVP, para calcular energías de absorción correspondientes a transiciones HOMO→LUMO. La solvatación en acetona se simuló usando el Modelo de Continuo Polarizable (PCM). Los espectros UV-Vis experimentales de Br_2 gaseoso mostraron picos de absorción a 238 nm ($\lambda_{1,exp}$) y 454 nm ($\lambda_{2,exp}$). Al disolverse en acetona, $\lambda_{2,exp}$ presentó un corrimiento hipsoacrómico que se observó a 395 y 365 nm para concentraciones de 0,04 y 0,01 M, respectivamente. Este cambio se atribuye a la formación de XBs, respaldado por espectros teóricos con picos a 390 nm (Br_2•••Ac) y 360 nm (Ac•••Br_2•••Ac). El pico a 238 nm se asocia con complejos Br_2•••Br_2, confirmado teóricamente a 240 nm. Un único pico a 415 nm en Br_2 diluido en aire se atribuye a complejos Br_2•••N_2, con pico teórico a 417 nm. La concordancia entre datos teóricos y experimentales valida la metodología y destaca el papel de los XBs en las propiedades espectrofotométricas del Br_2.

Palabras clave: enlaces de halógeno; espectrofotometría UV-Vis; modelado molecular; transiciones electrónicas.

Detecção e caracterização de ligações halógenas através de espectrofotometria UV-Vis e modelagem molecular

Resumo

Este estudo investiga as ligações de halogênio (XBs) em complexos de bromo e acetona (Br_2•••Ac) por meio de espectrofotometria UV-Vis e métodos computacionais. Realizaram-se cálculos de estrutura eletrônica, otimizações geométricas e estados excitados com o programa Gaussian 16. O método da teoria funcional da densidade dependente do tempo (TD-DFT) foi empregado, com o funcional M06-2X e o conjunto de base def2-TZVP, para calcular as energias de absorção correspondentes às transições HOMO→LUMO. A solvação em acetona foi simulada com o Modelo de Continuum Polarizável (PCM). Os espectros UV-Vis experimentais de Br_2 gasoso revelaram picos de absorção em 238 nm ($\lambda_{1,exp}$) e 454 nm ($\lambda_{2,exp}$). Ao ser dissolvido em acetona, $\lambda_{2,exp}$ apresentou um deslocamento hipsoacrômico, observandose em 395 e 365 nm para concentrações de 0,04 e 0,01 M, respectivamente. Esse deslocamento é atribuído à formação de XBs, sustentada por espectros teóricos com picos em 390 nm (Br_2•••Ac) e 360 nm (Ac•••Br_2•••Ac). O pico em 238 nm está relacionado a complexos Br_2•••Br_2, confirmado por cálculo teórico em 240 nm. Um único pico em 415 nm para Br_2 diluído em ar é atribuído a complexos Br_2•••N_2, com pico teórico em 417 nm. Os dados teóricos e experimentais mostram boa concordância, validando a metodologia e destacando o papel dos XBs nas propriedades espectrofotométricas do Br_2.

Palavras-chave: ligações de halogéneo; espectrofotometria UV-Vis; modelagem molecular; transições eletrônicas.

Introduction

Halogen bonds (XBs) have recently attracted considerable attention due to their distinctive characteristics and wide range of applications [1–3]. Typically, an XB is formed through an interaction between a covalently bonded halogen atom (X = I, Br, Cl, and, less commonly, F) and a Lewis base (B), represented as R–X•••B [4]. This type of interaction has been investigated in crystal structure analyses, which shows that the angle bond R–X•••B is approximately 180° [5, 6]. This is consistent with theoretical predictions [7, 8]. Furthermore, analyses of the molecular electrostatic potential (MEP) [8], the Laplacian of the electron density $L(\mathbf{r})$ [9, 10], and the potential acting on one electron in a molecule (PAEM) [11, 12] indicate that the electron density around the halogen atom is anisotropic. This anisotropy results in a region of depleted electron charge in the outer part of the R–X bond, known as the σ-hole, which facilitates the XB formation. Based on numerous studies employing MEP, the International Union of Pure and Applied Chemistry (IUPAC) has defined XBs as primarily electrostatic [13]. However, this definition is still subject of debate.

Despite the growing interest in XBs, there is a limited amount of research that directly correlates spectrophotometric data with theoretical chemistry parameters [14]. In 2006, Gogoi *et al.* [15] studied the XBs formed between 2-chloropyridine and iodine monochloride (ICl) in different solvent media, using ultraviolet-visible (UV-Vis) spectrophotometry and computational methods. Both their experimental and theoretical results confirmed that the absorption maximum (λ_{max}) is dependent on solvent polarity, with an observed blue shift explained by the formation of an XB between 2-chloropyridine and ICl. Analyses of Natural Bond Orbitals (NBO) [16], Natural Resonance Theory (NTR), and Quantum Theory of Atoms in Molecules (QTAIM) show an increase of the E_{int} as well as the covalent character with the solvent polarity. More recently, Xu and Guan explored the role of XBs in poly(vinylpyrrolidone)-I_2 (PVPI) chemistry using computational and experimental techniques, including UV-Vis spectrophotometry. They identified an XB between the carbonyl oxygen's lone pair and the σ-hole of I_2. In addition, iodide and iodine form various polyiodides via XBs, and iodine molecules can form iodine groups, also via XBs. The E_{int} of these XBs are less than −33 kJ mol^{-1}, which facilitates the release of I_2 molecules into the medium by PVPI, iodide, and polyiodide ions [17].

Bromine-acetone complex (Br_2•••Ac) is one known XB. Hassel and Strømme reported the first crystal structure of this XB when short Br•••O distances were found [6]. These interactions present an infinite double-chain assembly, with the Br_2 facing the lone pairs of nearest O atoms with a Br–Br•••O angle of 110°. The carbonyl groups and the Br_2 molecules are in the same plane. The Br_2 molecules showed a negligible bond elongation [$d_{Br\cdots Br}$ = 2.280 Å] in connection with pure bromine (Br) in the solid state [$d_{Br\cdots Br}$ = 2.286 Å]. Powel *et al.* determined the crystal structure of solid Br_2 at 250 K, using the neutron dust profile refinement technique [18]. Jones *et al.* in 2013 have used a combination of single-crystal X-ray (at 110 and 200 K) and high-resolution powder neutron diffraction (110 K only) to determine the crystal structure of the known Br_2•••Ac complex [19]. In these works, the authors have found several significant differences in geometrical parameters. For instance, the $d_{Br\cdots Br}$ in this XB shows an increase compared to the same molecule in the gas and crystalline phases. As the temperature increases, the length of this bond decreases, and this change seems to coincide with an increase in the $d_{Br\cdots O}$ with temperature. In addition, when acetone is deuterated (D = deuterium), a short C–D•••O distance is observed.

However, working with Br in the gas phase or solution is challenging due to its high reactivity, toxicity, and volatility. Moreover, its exothermic interaction with solvents like acetone requires additional precautions, especially due to its low boiling point of 58.8 °C [20]. Thus, the experimental characterization of Br_2•••Ac complexes in solution has not been exhaustively studied. Given these complexities and the limited correlation between spectrophotometric and theoretical data for XBs in literature, this study aims to provide a comprehensive investigation of Br_2•••Ac complexes using both UV-Vis spectrophotometry and computational methods. Specifically, the objectives are to experimentally characterize the UV-Vis spectral changes of Br and acetone, to attribute these changes to the formation of XBs supported by theoretical calculations, and to validate the combined experimental and computational methodology as an effective approach for detecting and characterizing XBs in different environments. This work seeks to enhance the understanding of how intermolecular interactions and electronic transitions influence the spectrophotometric properties of Br and provide a basis for future spectrophotometric XB studies.

Materials and Methods

Experimental Methods

Experimental UV-Vis spectra were performed on a UV-Vis spectrophotometer (SpectraMax M2e, USA) using SoftMax Pro 6.3 software. A vapor-tight quartz cell with 1 cm pitch length and 3 mL capacity was used. The wavelength range for the measurements was between 200 and 700 nm. Spectra of Br vapor [$Br_{2(g)}$], both saturated and mixed with air [$Br_{2(g)}$ + air], were analyzed. Additionally, measurements of Br_2 dissolved in acetone were performed at concentrations of 0.01 M [$Br_{2(dil)}$] and 0.04 M [$Br_{2(cc)}$]. Br (99.8%) and acetone (≥ 99.8%) were purchased from Sigma-Aldrich (Merck kGaA).

Computational Methods

Electronic structure calculations were performed using the Gaussian 16 program [21]. These calculations included geometry optimization, excited state, and energy calculations. All geometries were optimized using Time-Dependent Density Functional Theory (TD-DFT) with the M06-2X functional [22] and the def2-TZVP basis set [23]. M06-2X functional is recommended for the calculation of non-covalent interactions and electronic excitation energies [24, 25]. For all calculations, acetone solvation was simulated using the polarizable continuum model (PCM) [26, 27].

Theoretical UV-Vis absorption wavelengths (λ_{theor}) were obtained from TD-DFT calculations, performed with the same M06-2X functional and def2-TZVP basis set as used for geometry optimization. These calculations were carried out for isolated Br_2 and for the specific complexes Br_2•••Ac, Ac•••Br_2•••Ac, Br_2•••Br_2 and Br_2•••N_2 to simulate the different experimental conditions. The λ_{theor} values correspond to the maximum absorption calculated for the electronic transitions in these molecular systems.

Interaction energies (E_{int}) of the studied XBs were calculated with Eq. (1) to assess the stability of the formed complexes:

$$E_{int} = E_{AB} - (E_A + E_B) \qquad (1)$$

Where E_{AB} is the energy of the complex AB, and E_A and E_B are the energies of the monomers A and B, respectively. The calculated intermolecular distances were compared with the sum of the van der Waals radii to characterize the interactions.

To characterize the charge distribution and explore the nature of the interatomic interactions within the complexes, a topological analysis of the electron density [$\rho(\mathbf{r})$] was performed. The Quantum Theory of Atoms in Molecules (QTAIM) provides a framework to characterize the charge distribution of the molecular electron density [28]. Particularly, the topological analysis of the $L(\mathbf{r})$ function is an excellent tool to address a deep investigation of the electronic properties of a molecular system, allowing the exploration of inte-

ratomic interactions. The topology of the $L(\mathbf{r})$ function allows us to identify areas of concentration [$L(\mathbf{r}) > 0$] and depletion of electron charge [$L(\mathbf{r}) < 0$], and the localization of bond critical points (BCPs) and atomic interaction lines (AILs). This analysis helps to visualize and understand the Lewis acid-base nature of the interactions. QTAIM calculations were performed using the wave function obtained with Gaussian 16, and visualized with the AIMAll package [29].

Results and Discussion

Geometrical structures, intermolecular distances, and the E_{int} of the XBs studied are shown in **Figure 1**. The fully optimized geometries with bond angles Br–Br···Y (Y = Br, N, O) are always close to 180°. In all cases, the intermolecular equilibrium distances Br···Y are shorter than the sum of the van der Waals radii [30] of the interacting atoms [$r_{vdW(Br)} + r_{vdW(Y)}$]. This indicates that the Br···Y interactions are stabilizing. The Br···Y intermolecular distances ranges from 2.730 to 3.356 Å. These values agree with recently reported values for F–Br···Br–F (2.993 Å) and F–Br···Br–H (3.019 Å) complexes calculated at MP2/aug-cc-pVTZ level [31].

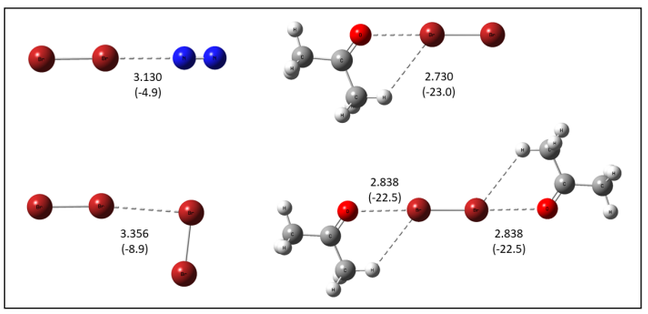

Figure 1. Geometrical structures of halogen bonds (XBs). The values of the O···Y (Y = N, O, Br) distances (in Armstrong) are given and the E_{int} (in kJ mol^{-1}) are in parentheses.

It is well established that XBs represent Lewis acid-base interactions [32]. Br_2 molecule can act as a Lewis acid in the axial regions, as is observed in **figure 1** with the N_2 molecule, the carbonyl O of acetone, and other Br_2 molecules. **Figure 1** also shows examples where the Br_2 molecule can act as a Lewis base in the equatorial region, for example, against another Br_2 molecule acting as an acid or against the H atoms of acetone. **Figure 2** illustrates the molecular graph and contour maps of the $L(\mathbf{r})$ function of the Br–Br···O=C$(CH_3)_2$ complex. It is well documented that regions of maximum charge concentration behave as Lewis bases, whereas regions of charge depression act as Lewis acids [33, 34].

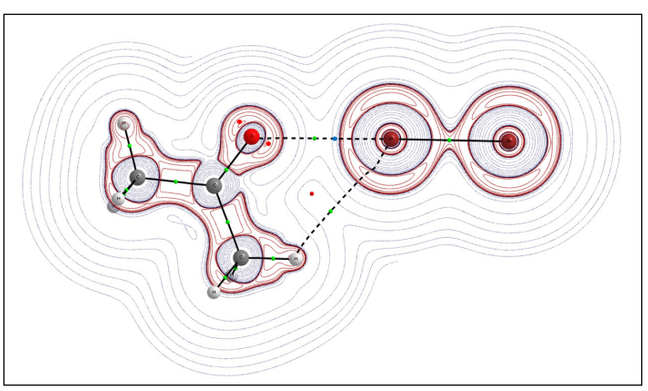

Figure 2. Contour maps of $L(\mathbf{r})$ for $(CH_3)_2C$=O···Br–Br complex. Red and blue dots indicate the locations of the maximum and minimum charge concentrations, respectively.

Figure 2 shows that between the carbonyl oxygen (C=O) and the Br atom there is a dotted line (AIL) with its corresponding bond critical point (BCP, green dot), an AIL and a BCP are also observed between a methyl hydrogen (CH_3) and the Br atom, indicating that there are bonding interactions between these atoms. In addition, **figure 2** also shows that the (C=O) exhibits two concentration maxima (red dots). One of these maxima is coordinated with the charge-depressed regions of the Br_2 molecule (blue dots). In other words, the principle of complementarity, as established by Bader [35], is observed, which tells us that maximum is coordinated with minimum of the $L(\mathbf{r})$ function.

Figure 3 displays the experimental spectra conducted in this study. It is observed that saturated gaseous Br_2 exhibits two distinct absorption peaks, namely $\lambda_{1,exp}$ = 238 nm and $\lambda_{2,exp}$ = 454 nm (green line, saturated $Br_{2(g)}$). These absorption peaks indicate specific wavelengths at which Br_2 strongly interacts with light. This finding suggests that concentrated $Br_{2(g)}$ has different energy levels associated with its electronic transitions, resulting in two distinct absorption bands. In contrast, when gaseous Br_2 is present in low concentrations with air [yellow line, $Br_{2(g)}$ + Air], a different absorption pattern emerges. In this case, only one absorption peak is observed: $\lambda_{2,exp}$ = 415 nm. The change in the absorption wavelength suggests that the electronic transitions of Br_2 molecules in lower concentrations are different from those observed in saturated $Br_{2(g)}$. This variation in absorption behavior could be attributed to changes in the electronic environment and intermolecular interactions as the concentration of Br_2 decreases. Similar vertical excitations have been found for molecular Br_2 in dilute carbon tetrachloride solution, with λ = 420 nm [36].

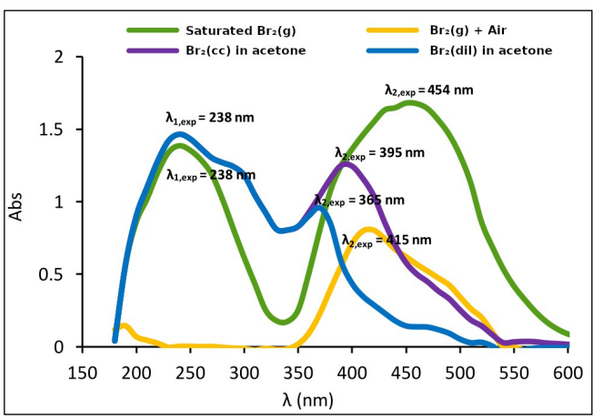

Figure 3. UV-Vis spectra of saturated $Br_{2(g)}$ (green line), $Br_{2(g)}$ diluted in air (yellow line), and Br_2 solutions in acetone at 0.04 M (purple line) and 0.01 M (blue line).

The spectra of Br_2 in acetone were obtained at the concentrations of 0.01 and 0.04 M ($Br_{2(cc)}$ and $Br_{2(dil)}$, respectively), which are presented in figure 3 through the blue and purple curves, respectively. At wavelengths below 350 nm, the curves for Br_2 in solution overlap with that for saturated $Br_{2(g)}$, maintaining a $\lambda_{1,exp}$ of 238 nm. However, this same $\lambda_{1,exp}$ is not observed in the case of $Br_{2(g)}$ + Air, suggesting that Br_2 does not interact with the gasses present in the air as it does with itself at higher concentrations (in the case of saturated $Br_{2(g)}$) or with acetone molecules of the environment in solution. At wavelengths longer than 350 nm, a shift of $\lambda_{2,exp}$ towards shorter wavelengths is observed, which accompanies as Br_2 is diluted in acetone, showing values of $\lambda_{2,exp}$ = 454, 395 and 365 nm for saturated $Br_{2(g)}$, $Br_{2(cc)}$, and $Br_{2(dil)}$, respectively. A decrease in the peak height of λ_{max} is also observed, which is characteristic of a dilution of the molecules of Br_2 in the environment.

The results observed in **figure 3** suggest that the solvent environment (acetone, in this case) influences the electronic transitions of Br_2 molecules, causing a modification in their absorption behaviour. The observed changes in the absorption wavelengths provide valuable information on the interactions that may exist between Br_2 and the solvent molecules, whether the latter is acetone or other molecules in the gas-phase environment.

Figure 4 shows the molecular orbitals corresponding to the characteristic electronic transitions of molecular Br_2 (**figure 4A**) and of the $Br_2\cdots Br_2$, $Br_2\cdots Ac$, and $Ac\cdots Br_2\cdots Ac$ complexes (**figures 4B**, **4C**, and **4D**, respectively), together with their respective absorption maxima (λ_{theor}). The theoretical results reveal that the presence of $\lambda_{1,exp}$ = 238 nm of saturated $Br_{2(g)}$ (green line in **figure 1**) is attributed to the formation of XBs between molecules of the same gas (see **figure 4B**), with a $\lambda_{1,theor}$ = 240 nm. Furthermore, the observed $\lambda_{2,exp}$ shift between saturated $Br_{2(g)}$ ($\lambda_{2,exp}$ = 454 nm), $Br_{2(cc)}$ ($\lambda_{2,exp}$ = 395 nm), and $Br_{2(dil)}$ ($\lambda_{2,exp}$ = 365 nm) correlates with the number of XBs formed between Br_2 and acetone, where λ_{theor} = 444 nm for the Br_2 molecule (without XB), $\lambda_{2,theor}$ = 390 nm for the $Br_2\cdots Ac$ complex (with 1 XB) and $\lambda_{2,theor}$ = 360 nm for the $Ac\cdots Br_2\cdots Ac$ complex (with 2 XBs). The geometric structures found theoretically for $Br\cdots O$ interactions (see **figure 1**) are similar to those reported by Nenajdenko *et al.* [37].

The λ_{theor} were calculated for a series of $Br_2\cdots(Ac)_n$ complexes with n = 0–6, where the maximum number of XBs observed was two between Br_2 and acetone. These XBs can only be formed by the axial regions of the Br_2 molecule with the free O pair of the acetone ($Br–Br\cdots O{=}C$). The rest of the interactions observed in the complexes obtained correspond to hydrogen bonds (HBs) that are established by the equatorial region of each Br atom (results not presented). However, regardless of the complex considered, it was observed that the λ_{theor} only varies with the number of XBs formed. In figure 4 only the electronic transitions most relevant between $Br_2\cdots Br_2$ and $Br_2\cdots Ac$ complexes, with one XB (**figure 4B** and **4C**) and with two XBs (**figure 4D**), are presented.

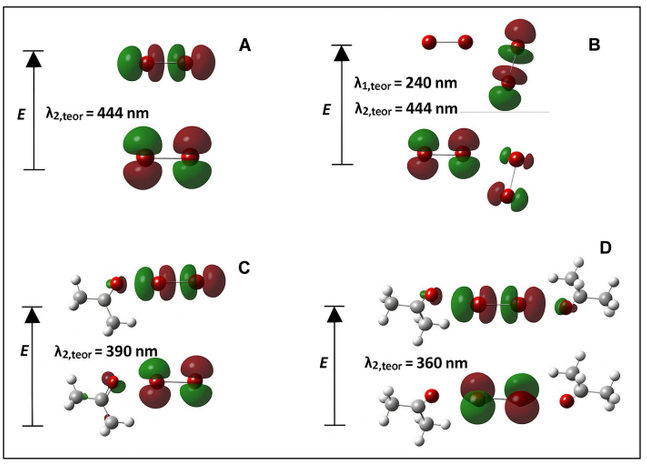

Figure 4. Canonical Highest Occupied Molecular Orbital (HOMO) and Lowest Unoccupied Molecular Orbital (LUMO) of Br_2 (A), of $Br_2\cdots Br_2$ (B), $Br_2\cdots Ac$ (C), and $Ac\cdots Br_2\cdots Ac$ (D) complexes, with their respective theoretical λ_{max}.

The $Br_2\cdots Br_2$ complex (**figure 4B**) presents a similar characteristic λ_{theor} of an isolated Br_2 molecule (444 nm in **figure 4A**), which is in reasonable agreement with saturated $Br_{2(g)}$ presented with a green line in **figure 3** ($\lambda_{2,exp}$ = 454 nm). However, none of the electronic transitions shown in figure 4 can explain the experimental UV-Vis spectrum of $Br_{2(g)}$ + air (yellow line in **figure 3**). Considering that air contains 78% $N_{2(g)}$, the complex $Br_2\cdots N_2$ was chosen as the simulation molecular system, whose Highest Occupied Molecular Orbital (HOMO) and Lowest Unoccupied Molecular Orbital (LUMO) are presented in figure 5 together with the characteristic λ_{theor} value of 417 nm. This result agrees with the λ_{exp} of $Br_{2(g)}$ + Air (415 nm). It is crucial to highlight that in the $Br_2\cdots Br_2$ complex, the electronic transition takes place in the Br_2 monomer, which serves as a Lewis acid. This is much more visible in the other complexes.

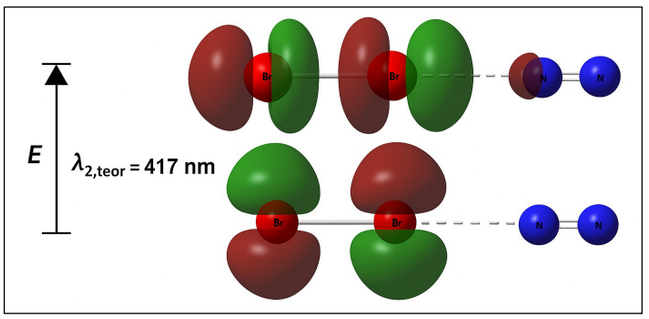

Figure 5. Canonical Highest Occupied Molecular Orbital (HOMO) and Lowest Unoccupied Molecular Orbital (LUMO) of the $Br_2\cdots N_2$ complex with its respective characteristic λ_{theor}.

Table 1 summarizes the values of the experimental ($\lambda_{i,exp}$) and theoretical ($\lambda_{i,theor}$) absorption maxima obtained for each system studied, with their respective percentage errors [$\varepsilon_{\%}(\lambda_i)$], calculated using Eq. (2).

$$\varepsilon_{\%}(\lambda_i) = \frac{|\lambda_{i,theor} - \lambda_{i,exp}|}{\lambda_{i,exp}} 100 \qquad (2)$$

Where $\lambda_{i,exp}$ and $\lambda_{i,theor}$ represent the absorption wavelengths of the experimentally and theoretically observed peaks, respectively, for system *i*. The $\varepsilon_{\%}(\lambda_i)$ values show errors of less than 3%, indicating that the molecular systems used as models successfully reproduce the experimental UV-Vis spectra.

Table 1. Experimental and theoretical absorption maxima obtained for each system studied.

System	Simulation	$\lambda_{1,exp}$ (nm)	$\lambda_{1,theor}$ (nm)	$\varepsilon_{\%}(\lambda_i)$ (%)	$\lambda_{2,exp}$ (nm)	$\lambda_{2,theor}$ (nm)	$\varepsilon r\%(\lambda_2)$ (%)
$Br_{2(g)}$	$Br_2\cdots N_2$	238	240	0.8	454	444	2.2
$Br_{2(g)}$ + Air	$Br_2\cdots Br_2$	-	-	-	415	417	0.5
$Br_{2(dil)}$	$Br_2\cdots Ac$	238	240	0.8	395	390	1.3
$Br_{2(cc)}$	$Ac\cdots Br_2\cdots Ac$	238	240	0.8	365	360	1.4

$\lambda_{1,exp}$: Experimental maxima wavelengths.
$\lambda_{1,theor}$: Theoretical maxima wavelengths, obtained from the systems used as models to reproduce the spectrum of each simulation.
$\varepsilon_{\%}(\lambda_i)$: Values of the percentage error.

The results of these experimental studies contribute to our understanding of the spectrophotometric properties of Br_2 and its behaviour in different states and environments. The change in absorption wavelengths at different concentrations and environments highlights the importance of intermolecular interactions and electronic factors in determining the spectrophotometric properties of Br_2. This information can help to interpret the experimental data and lay the foundation for future research and applications related to Br_2 in different environments. Finally, there are strong correlations between the experimental and theoretical results, indicating that the methodology employed in this work could be applied to the detection and characterization of certain XBs present both in the gas phase and in solution.

Conclusions

Experimental UV-Vis spectra revealed two distinct absorption peaks for saturated gaseous Br_2, specifically at 238 nm ($\lambda_{1,exp}$) and 454 nm ($\lambda_{2,exp}$). Upon dissolution and dilution in acetone, at concentrations of 0.04 and 0.01 M, a significant hypsochromic shift (towards shorter wavelengths) of $\lambda_{2,exp}$ was observed, shifting to 395 and 365 nm, respectively. These experimental shifts are strongly correlated with the formation of XBs between Br_2 and acetone molecules, as evidenced by our theoretical simulations.

The strong agreement between experimental and theoretical absorption maxima obtained for all studied systems, with percentage of errors typically less than 3%, solidly validates the combined experimental UV-Vis spectrophotometry and computational methodology employed in this study for detecting and characterizing XBs in different environments. This work effectively demonstrates the clear effect of XBs on the UV-Vis absorption spectrum of Br_2 in various media.

Finally, our findings underscore the importance of integrating experimental and computational approaches for exploring and understanding subtle non-covalent interactions, providing a foundation for further studies on other halogenated compounds and their potential applications.

Acknowledgements

The authors gratefully acknowledge the financial support from the Consejo Nacional de Investigaciones Científicas y Técnicas (CONICET-Argentina) and Secretaría General de Ciencia y Técnica de la Universidad Nacional del Nordeste (SGCyT-UNNE) (PI-22V002). M.O.M. is a research fellow of CONICET.

References

[1] G. Cavallo *et al*., "The halogen bond," *Chem Rev*, vol. 116, no. 4, pp. 2478–2601, 2016. DOI: https://doi.org/10.1021/acs.chemrev.5b00484.

[2] P. Politzer, P. Lane, M. C. Concha, Y. Ma, and J. S. Murray, "An overview of halogen bonding," *J Mol Model*, vol. 13, pp. 305–311, 2007.

[3] H. Yang and M. W. Wong, "Application of halogen bonding to organocatalysis: A theoretical perspective," *Molecules*, vol. 25, no. 5, p. 1045, 2020.

[4] P. Metrangolo and G. Resnati, "Halogen bonding: a paradigm in supramolecular chemistry," *Chemistry–a European journal*, vol. 7, no. 12, pp. 2511–2519, 2001. DOI: https://doi.org/10.1002/1521-3765(20010618)7:12 <2511::AID-CHEM25110<3.0.CO;2-T.

[5] P. Metrangolo, H. Neukirch, T. Pilati, and G. Resnati, "Halogen bonding based recognition processes: a world parallel to hydrogen bonding," *Acc Chem Res*, vol. 38, no. 5, pp. 386–395, 2005. DOI: https://doi.org/10.1021/ar0400995.

[6] O. Hassel, K. O. Strømme, E. Stenhagen, G. Andersson, E. Stenhagen, and H. Palmstierna, "Crystal structure of the 1:1 addition compound formed by acetone and bromine," *Acta Chem. Scand*, vol. 13, no. 2, pp. 275–280, 1959. DOI: https://doi.org/10.3891/acta.chem.scand.13-0275.

[7] L. P. Wolters, P. Schyman, M. J. Pavan, W. L. Jorgensen, F. M. Bickelhaupt, and S. Kozuch, "The many faces of halogen bonding: A review of theoretical models and methods," *Wiley Interdiscip Rev Comput Mol Sci*, vol. 4, no. 6, pp. 523–540, 2014. DOI: https://doi.org/10.1002/wcms.1189.

[8] P. Politzer, J. S. Murray, and T. Clark, "Halogen bonding and other <-hole interactions: A perspective," *Physical Chemistry Chemical Physics*, vol. 15, no. 27, pp. 11178–11189, 2013. DOI: https://doi.org/10.1039/c3cp00054k.

[9] K. Eskandari and H. Zariny, "Halogen bonding: A lump–hole interaction," *Chem Phys Lett*, vol. 492, no. 1–3, pp. 9–13, 2010. DOI: https://doi.org/10.1016/j.cplett.2010.04.021.

[10] D. J. R. Duarte, E. L. Angelina, and N. M. Peruchena, "On the strength of the halogen bonds: mutual penetration, atomic quadrupole moment and Laplacian distribution of the charge density analyses," *Comput Theor Chem*, vol. 998, pp. 164–172, 2012. DOI: https://doi.org/10.1016/j.comptc.2012.07.019.

[11] E. Bartashevich and V. Tsirelson, "A comparative view on the potential acting on an electron in a molecule and the electrostatic potential through the typical halogen bonds," J *Comput Chem*, vol. 39, no. 10, pp. 573–580, 2018. DOI: https://doi.org/10.1002/jcc.25112.

[12] D. J. R. Duarte, G. J. Buralli, and N. M. Peruchena, "Is σ-hole an electronic exchange channel in YX⋯ CO interactions?," *Chem Phys Lett*, vol. 710, pp. 113–117, 2018. DOI: https://doi.org/10.1016/j.cplett.2018.08.060.

[13] G. R. Desiraju *et al*., "Definition of the halogen bond (IUPAC Recommendations 2013)," *Pure and applied chemistry*, vol. 85, no. 8, pp. 1711–1713, 2013. DOI: https://doi.org/10.1351/PAC-REC-12-05-10.

[14] R. Shi, D. Yu, F. Zhou, J. Yu, and T. Mu, "An emerging deep eutectic solvent based on halogen-bonds," *Chemical Communications*, vol. 58, no. 29, pp. 4607–4610, 2022. https://doi.org/10.1039/D2CC00745J.

[15] P. Gogoi, U. Mohan, M. P. Borpuzari, A. Boruah, and S. K. Baruah, "UV-Visible spectroscopy and density functional study of solvent effect on halogen bonded charge-transfer complex of 2-Chloropyridine and iodine monochloride," *Arabian Journal of Chemistry*, vol. 12, no. 8, pp. 4522–4532, 2019. DOI: https://doi.org/10.1016/j.arabjc.2016.07.011.

[16] A. E. Reed, L. A. Curtiss, and F. Weinhold, "Intermolecular interactions from a natural bond orbital, donor-acceptor viewpoint," *Chem Rev*, vol. 88, no. 6, pp. 899–926, 1988. DOI: https://doi.org/10.1021/cr00088a005.

[17] X. Xu and Y. Guan, "Investigating the complexation and release behaviors of iodine in Poly (vinylpyrrolidone)-Iodine systems through experimental and computational approaches," *Ind Eng Chem Res*, vol. 59, no. 52, pp. 22667–22676, 2020. DOI: https://doi.org/10.1021/acs.iecr.0c04766.

[18] B. M. Powell, K. M. Heal, and B. H. Torrie, "The temperature dependence of the crystal structures of the solid halogens, bromine and chlorine," *Mol Phys*, vol. 53, no. 4, pp. 929–939, 1984. DOI: https://doi.org/10.1080/00268978400102741.

[19] R. H. Jones, K. S. Knight, W. G. Marshall, S. J. Coles, P. N. Horton, and M. B. Pitak, "The competition between halogen bonds (Br center dot center dot center dot O) and CH center dot center dot center dot O hydrogen bonds: the structure of the acetone-bromine complex revisited," *CrystEngComm*, vol. 15, no. 42, pp. 8572–8577, 2013. DOI: https://doi.org/10.1039/c3ce41472h.

[20] D. L. Perry, *Handbook of inorganic compounds*. CRC press, 2016.

[21] M. J. Frisch et al., "Gaussian˜16 Revision C.01," 2016.

[22] Y. Zhao and D. G. Truhlar, "The M06 suite of density functionals for main group thermochemistry, thermochemical kinetics, noncovalent interactions, excited states, and transition elements: two new functionals and systematic testing of four M06-class functionals and 12 other functionals," *Theor Chem Acc*, vol. 120, no. 1, pp. 215–241, 2008. DOI: https://doi.org/10.1007/s00214-007-0310-x.

[23] J.-D. Chai and M. Head-Gordon, "Long-range corrected hybrid density functionals with damped atom–atom dispersion corrections," *Physical Chemistry Chemical Physics*, vol. 10, no. 44, pp. 6615–6620, 2008. DOI: https://doi.org/10.1039/B810189B.

[24] W. Kohn, A. D. Becke, and R. G. Parr, "Density functional theory of electronic structure," *J Phys Chem*, vol. 100, no. 31, pp. 12974–12980, 1996. DOI: https://doi.org/10.1021/jp960669l.

[25] B. P. Pritchard, D. Altarawy, B. Didier, T. D. Gibson, and T. L. Windus, "New basis set exchange: An open, up-to-date resource for the molecular sciences community," *J Chem Inf Model*, vol. 59, no. 11, pp. 4814–4820, 2019. DOI: https://doi:10.1021/acs.jcim.9b00725.

[26] E. Cancès, B. Mennucci, and J. Tomasi, "A new integral equation formalism for the polarizable continuum model: Theoretical background and applications to isotropic and anisotropic dielectrics," *J Chem Phys*, vol. 107, no. 8, pp. 3032–3041, 1997. DOI: https://doi.org/10.1063/1.474659.

[27] J. Tomasi, B. Mennucci, and R. Cammi, "Quantum mechanical continuum solvation models," *Chem Rev*, vol. 105, no. 8, pp. 2999–3094, 2005. DOI: https://doi.org/10.1021/cr9904009.

[28] F. Richard and R. Bader, "Atoms in molecules: a quantum theory," 1990, Oxford University Press, Oxford.

[29] Á. M. Pendás and C. Gatti, "Quantum theory of atoms in molecules and the AIMAll software," *Complement. Bond. Anal*, vol. 43, 2021.

[30] A. van Bondi, "van der Waals Volumes and Radii," *J Phys Chem*, vol. 68, no. 3, pp. 441–451, 1964. DOI: https://doi.org/10.1021/j100785a001.

[31] D. J. R. Duarte, G. L. Sosa, N. M. Peruchena, and I. Alkorta, "Halogen bonding. The role of the polarizability of the electron-pair donor," *Physical Chemistry Chemical Physics*, vol. 18, no. 10, pp. 7300–7309, 2016.

[32] G. J. Buralli, D. J. R. Duarte, G. L. Sosa, and N. M. Peruchena, "Lewis acid-base behavior of hypervalent halogen fluorides in gas phase," *Struct Chem*, vol. 28, pp. 1823–1830, 2017. DOI: https://doi.org/10.1007/s11224-017-0973-5.

[33] S. J. Grabowski, "Halogen bonds with carbenes acting as Lewis base units: complexes of imidazol-2-ylidene: theoretical analysis and experimental evidence," *Physical Chemistry Chemical Physics*, vol. 25, no. 13, pp. 9636–9647, 2023. DOI: https://doi.org/10.1039/D2CP05046K.

[34] P. R. Varadwaj, "Halogen Bond via an Electrophilic ϖ-Hole on Halogen in Molecules: Does It Exist?," *Int J Mol Sci*, vol. 25, no. 9, p. 4587, 2024. DOI: https://doi.org/10.3390/ijms25094587.

[35] R. F. W. Bader, P. L. A. Popelier, and C. Chang, "Similarity and complementarity in chemistry," *Journal of Molecular Structure: THEOCHEM*, vol. 255, pp. 145–171, 1992. DOI: https://doi.org/10.1016/0166-1280(92)85008-4.

[36] S. Hubinger and J. B. Nee, "Absorption spectra of Cl2, Br2 and BrCl between 190 and 600 nm," *J Photochem Photobiol A Chem*, vol. 86, no. 1–3, pp. 1–7, 1995. DOI: https://doi.org/10.1016/1010-6030(94)03947-F.

[37] V. G. Nenajdenko *et al*., "Structural organization of dibromodiazadienes in the crystal and identification of Br••• O halogen bonding involving the nitro group," *Molecules*, vol. 27, no. 16, p. 5110, 2022. DOI: https://doi.org/10.3390/molecules27165110.

Citación del artículo:

C. A. Galarza, M. O. Miranda, and D. J. R. Duarte, "Detection and characterization of halogen bonds by UV-Vis spectrophotometry and molecular modelling", *Rev. Colomb. Quim.*, vol. 53, no. 2, pp. 13–18, 2024. DOI: https://doi.org/10.15446/rev.colomb.quim.v53n2.116648